Journal of Materials Chemistry

Cite this: J. Mater. Chem., 2012, 22, 17954

www.rsc.org/materials

PAPER

Construction of glycoprotein multilayers using the layer-by-layer assembly technique

Bo Wang,[ab] Zhiyong Liu,[c] Yanli Xu,[c] Yuhua Li,[a] Tiezhu An,*[a] Zhaohui Su,[b] Bo Peng,[b] Yuan Lin*[b] and Qian Wang[d]

Received 15th May 2012, Accepted 11th July 2012
DOI: 10.1039/c2jm33070a

A novel glycoprotein film was assembled from pig gastric mucin and poly(acrylamide-*co*-3-acrylamidophenylboronic acid) using a layer-by-layer technique, driven by the formation of boronate ester bonds between the boronic acid units and the polyols. The assembly was monitored by quartz crystal microbalance and UV-vis spectroscopy. The film thickness is increased with increasing the ionic strength and the pH of assembly solutions. Furthermore, the dynamic response of the assembled film to the presence of glucose was monitored in real time using quartz crystal microbalance with dissipation. Glucose competes with pig gastric mucin to bind with the boronic acid units in the multilayer film, resulting in its disassembly, and the disassembly rate is a function of the glucose concentration. The film is also sensitive to glucose at physiological conditions, albeit the response is weaker and slower than that at higher pH. This glucose-sensitive glycoprotein multilayer film can therefore be applied in glucose sensing and self-regulated insulin release systems.

Introduction

In this paper, we report a novel glucose-sensitive glycoprotein film assembled by the layer-by-layer (LbL) technology. A phenylboronic acid (PBA) tailored random copolymer was used, which could generate covalent boronate ester linkages with glycoproteins and lead to the formation of stable glycoprotein multilayer films. The PBA units in the film can form reversible complexes with diol-containing molecules, such as polyols, carbohydrates and sugar residues located on the surface of glycoproteins in aqueous media.[1–4] The mechanism of the reaction is the formation of a heterocyclic diester from 1,2- or 1,3-diol groups and a tetrahedral boronate ion.[5] Up to now, PBA-bearing polymers have found extensive applications in sensor technology,[6,7] drug delivery,[8] and affinity chromatography.[9]

Mucins are highly charged and heavily glycosylated proteins, which are present at the mucosal surfaces of animal epithelia.[10] These glycosylated proteins are parts of the protective epithelial mucus layer that plays an important role as an anti-adhesive barrier to selective substances between the host and external environment.[11,12] Based on their excellent biological and physicochemical properties, mucins have been applied in the surface modification of biomaterials over a number of years.[13,14]

LbL technology is a facile and versatile method, which can provide precise control of the film thickness at the nanometer scale and of the properties of the resultant films.[15] Conventionally electrostatic interactions are the main driving force for LbL assembly.[16–18] In general, the mild process of LbL assembly can maintain the natural architectures of biomolecules,[19,20] thus making it a good method for fabricating functional biocompatible films. Recently, a variety of non-electrostatic interactions including hydrogen bonding, hydrophobic interactions, ion–dipole interactions and biospecific recognition were employed in the LbL assembly.[18,21,22] Some studies have shown that the interaction between PBA and polyols, such as polysaccharide mannan and poly(vinyl alcohol) (PVA),[23,24] can be used to construct ultrathin films by the LbL method. In this work, we used pig gastric mucin (PGM) and poly(acrylamide-*co*-3-acrylamidophenylboronic acid) [P(AAm-AAPBA)] to construct LbL multilayer films driven by the formation of boronate ester bonds between the boronic acid units and the polyols. Furthermore, as the boronate ester bonding is reversible, the resultant films are glucose-sensitive in aqueous solutions.

Quartz crystal microbalance with dissipation monitoring (QCM-D) is a real-time and label-free method for monitoring intermolecular interactions on various surfaces based on analyzing the variation of the quartz crystal frequency (f) and the energy dissipation (D).[25–28] This method is highly sensitive for *in situ* real-time analysis, therefore QCM-D has been broadly applied to analyze the adsorption profile of proteins or plant viruses,[29–31] formation of polymer films[32,33] and cell adhesion and

[a]*College of Life Science, Northeast Forestry University, Harbin 150040, P.R. China*
[b]*State Key Laboratory of Polymer Physics and Chemistry, Changchun Institute of Applied Chemistry, Chinese Academy of Sciences, Changchun 130022, P.R. China. E-mail: linyuan@ciac.jl.cn; Fax: +86-431-85262126; Tel: +86-431-85262658*
[c]*Northeast Institute of Geography and Agroecology, Chinese Academy of Sciences, Changchun 130012, P.R. China*
[d]*Department of Chemistry and Biochemistry, University of South Carolina, 631 Sumter Street, Columbia, South Carolina 29208, USA*

spreading.[34–38] In the present study, we sought to characterize the disassembly kinetics of a LbL assembly film in response to glucose using QCM-D, which enables us to quantitatively describe the interactions between carbohydrates (such as glucose) and PBA groups in the assembly film. Furthermore, the additional benefit of measuring the dissipation of the disintegrating process makes it possible to investigate the viscoelastic properties and structure of the multilayer films.

Experimental section

Materials

Poly(acrylamide-*co*-3-acrylamidophenylboronic acid) [P(AAm-AAPBA)] was synthesized as reported.[39] Poly(diallyldimethylammonium chloride) (PDDA, M_W = ~200 000–350 000) and poly(sodium 4-styrene sulfonate) (PSS, M_W = 70 000) were purchased from Sigma-Aldrich Co.; Pig gastric mucin (PGM, M_W 9 × 10^6) was purchased from Shanghai Yuanye Biotechnology Co., Ltd. All the chemicals were used as received without further purification. Water was purified using a UNIQUE-R20 system (18.2 MΩ). Silver electrodes (Model 49U-C20SSA-9MHz) were manufactured by Beijing Ziweixing Microelectronic Co., Ltd.

Characterization

The LbL assembly process of PGM and P(AAm-AAPBA) was monitored by a Protek Frequency Counter (Model C3100) and UV-vis absorption spectrometer (Beijing Purkinje General Instrument Co., Ltd, Model TU-1901). The dynamic response behavior of the assembly films in the presence of glucose was monitored with a quartz crystal microbalance with dissipation monitoring (QCM-D, Q-Sense E1, Sweden) equipped with a QFM 401 flow module. The morphology of the PGM/P(AAm-AAPBA) film was obtained using an Agilent 5500 atomic force microscopy (AFM) instrument (Agilent Technologies Co., Ltd) operating in tapping mode.

Fabrication of LbL multilayer film from PGM and P(AAm-AAPBA)

The LbL formation of PGM and P(AAm-AAPBA) was conducted according to the following procedure. Firstly a substrate (silver-coated electrode or quartz slide) was immersed in a PDDA solution (1 mg mL^{-1}, containing 0.25 M NaCl) for 15 min, and then washed thoroughly with deionized water, followed by drying with nitrogen gas. The substrate coated with positively charged PDDA was immersed in a PSS solution (1 mg mL^{-1}, containing 0.25 M NaCl) for 15 min. Again the substrate was washed thoroughly with deionized water and dried with nitrogen gas. This alternate cycle was repeated twice and an additional PDDA layer was coated as the outermost surface to construct the precursor film $(PDDA/PSS)_2$/PDDA, where the numerical value two indicates the number of polymer bilayers. The precursor film provides uniform charge and a smooth surface for subsequent deposition.

PGM and P(AAm-AAPBA) solutions were prepared by dissolving the corresponding materials in phosphate-buffered saline (PBS) (0.01 M, pH 9.0, containing 0.5 M NaCl), and the final concentrations were both 0.1 mg mL^{-1}. The substrate overlaid with a $(PDDA/PSS)_2$/PDDA precursor film was alternately immersed in a PGM solution for 30 min and then in a P(AAm-AAPBA) solution for another 30 min. After each immersion step the substrate was rinsed with PBS buffer and dried with nitrogen gas. The assembly process was monitored using quartz crystal microbalance (QCM) and UV-vis spectroscopy.

QCM-D measurements

The dynamic response behavior of the assembly films in the presence of glucose was characterized using a QCM-D equipped with a QFM 401 flow module. The sensor was an AT-cut quartz crystal coated with gold on each side with a fundamental resonance frequency of 5 MHz (QSX 301, Q-Sense AB, Sweden). In brief, the QCM-D technique monitors simultaneously both the shifts of frequency (Δf) and dissipation (ΔD) in response to adsorption of materials on the surface of the crystal sensor. The quartz crystal frequency is directly related to the amount of mass deposited on the sensor surface, and the energy dissipation is related to the viscoelastic properties of the adlayers. The voltage applied over the crystal results in a thickness shear mode oscillation. The oscillation is driven at the crystal's fundamental frequency or an overtone. QCM-D records the frequencies at the first, third, fifth, seventh, ninth, eleventh and thirteenth overtone (5, 15, 25, 35, 45, 55 and 65 MHz, respectively), in which the third overtone often is the most stable one. Therefore we registered the frequency and the dissipation changes in third overtone frequency during our experiments. For rigid films, there is a linear relationship between the amount of mass adsorbed onto the crystal surface (normally in the 1 ng cm^{-2} range)[40] and the frequency shift of the crystal in air or vacuum according to the Sauerbrey equation[41]

$$\Delta m = -\frac{\rho_q l_q}{f_0}\frac{\Delta f}{n}$$

where f_0 is the fundamental frequency, and l_q and ρ_q are the thickness and density of the quartz crystal, respectively. n represents the overtone number, which is an odd number ($n = 1$, 3, 5, 7, 9, 11, 13). This Sauerbrey equation is also applied in the situation of liquids although the adsorbed mass includes the amount of coupled water. The dissipation factor (D) is related to the structure and viscoelastic properties of the adlayers. ΔD, is defined as[42]

$$\Delta D = \frac{E_{\text{dissipated}}}{2\pi E_{\text{stored}}}$$

where $E_{\text{dissipated}}$ is energy dissipated during one period of oscillation and E_{stored} is the energy stored in the oscillating system. The measurement of ΔD is based on the fact that the voltage over the crystal decays exponentially as a damped sinusoidal when the driving power of the piezoelectric oscillator is switched off.[42]

A piece of gold sensor was cleaned in an aqueous mixture of ammonium hydroxide and hydrogen peroxide ($NH_3 \cdot H_2O/H_2O_2/H_2O$ = 1/1/5, v/v/v) at 75 °C for 30 min, and then the sensor was rinsed thoroughly with deionized water and dried with nitrogen gas. (**Caution**: the ammonium peroxide mix solution should be used in a fume hood, with proper protection). Thereafter, all tubing was cleaned with 2% SDS for 30 min, and thoroughly

rinsed with deionized water. The gold sensor coated with (PGM/P(AAm-AAPBA))$_6$ film was installed into the QFM 401 flow module and the system was equilibrated at 25 ± 0.01 °C with degassed PBS (pH 9.0) buffer until the baseline was stable. After that, glucose solution at different concentrations in PBS (pH 9.0) was injected. To study the response of glucose to the assembly film in physiological conditions, the shifts of frequency and energy dissipation were measured by injecting PBS (pH 7.4) containing 1 mg mL^{-1} glucose.

AFM imaging

AFM imaging measurements were performed in ambient conditions using an Agilent 5500 atomic force microscopy instrument with tapping mode. Silicon tips with a resonance frequency of ~300 Hz, a spring constant of about 2 N m^{-1} and a scan rate of 1 Hz were used. The new silicon wafers were cleaned with H_2SO_4/H_2O_2 (7/3, v/v) solution at 75 °C, then sonicated three times in deionized water and dried with nitrogen gas before assembly. (PGM/P(AAm-AAPBA))$_6$ film was fabricated on silicon wafers as described previously. Then the coated silicon wafers were immersed into two different pH values of PBS (pH 7.4 and 9.0) glucose solution for 10 min at 25 °C respectively. After that the wafers were rinsed with deionized water and dried with nitrogen gas before testing. The root mean square (RMS) roughness of the sample was calculated after second order flattening using Picoimage software.

Results and discussion

Fabrication of PGM and P(AAm-AAPBA) multilayer film

It is well-known that the isoelectric point (pI) of PGM is ~2–3,[11] so that PGM can be considered as an anionic macromolecule at pH 9.0. In the present study, the first layer of PGM was deposited as a result of electrostatic interaction between the anionic PGM and cationic PDDA surface. After that, the surface carries a lot of hydroxy groups, which can bind with P(AAm-AAPBA) by covalent boronate ester bonding. The outermost surface restores a PBA-rich surface for the next layer deposition. The alternated deposition of PGM and P(AAm-AAPBA) was repeated to construct the LbL multilayer film. This process is depicted schematically in Scheme 1.

A silver electrode, which was an AT-cut quartz crystal (9 mm in diameter) coated with silver (4.5 mm in diameter) on each side with a resonance frequency of 9 MHz, was cleaned with deionized water, dried with nitrogen gas and used in the QCM analysis. QCM data for PGM and P(AAm-AAPBA) depositions are presented in Fig. 1. For each newly adsorbed PGM/P(AAm-AAPBA) bilayer on silver electrodes, the average of the frequency shift was 257 ± 103 Hz, which corresponded to 112 ± 45 ng and 3.51 ± 1.41 nm of PGM/P(AAm-AAPBA) on each side of the electrode calculated by Sauerbrey's equation.[41] The UV spectra of P(AAm-AAPBA) and PGM in aqueous solution are shown in Fig. 2a, and the UV spectra of the assembly film constructed with different dipping cycles are shown in Fig. 2b. The peak at 245 nm is assigned to the absorbance of the P(AAm-AAPBA) moiety of the composite film, which increases linearly along with the increase of the cycles of P(AAm-AAPBA) deposition (Fig. 2c). Both the QCM and UV data indicate that the deposition process is successful and reproducible from layer to layer.

The effect of different parameters on the LbL assembly process

To study the effect of ionic strength on assembly film formation, PGM/P(AAm-AAPBA) multilayer films were fabricated in 0.01 M PBS at pH 9.0 with various concentrations of NaCl. As shown in Fig. 3, the amount of film materials deposited on the electrode increases when the salt concentration increases from 0 M to 0.5 M. The rising shift of frequency, corresponding to the increase of bilayers, indicates the sequential deposition of materials. After 10 adsorption cycles, the masses of assembly materials adsorbed on each side of the silver electrodes were 0.55 ± 0.02 μg (0 M NaCl), 0.59 ± 0.01 μg (0.15 M NaCl), 0.69 ± 0.06 μg (0.25 M NaCl) and 1.07 ± 0.08 μg (0.5 M NaCl), respectively. It confirms that the adsorbed amount of materials onto the multilayer film can be controlled by the ionic strength. The rational effect of salt is that the addition of inorganic salt can reduce the repulsion between phenylboronate ions and

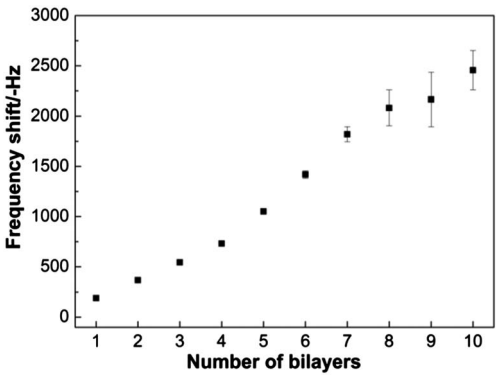

Fig. 1 Bilayer deposition of PGM and P(AAm-AAPBA) on the (PDDA/PSS)$_2$/PDDA-coated silver electrode monitored by QCM. The subscript denotes the number of bilayers deposited. The concentrations of PGM and P(AAm-AAPBA) were both 0.1 mg mL^{-1} in 0.01 M PBS (pH 9.0) containing 0.5 M NaCl.

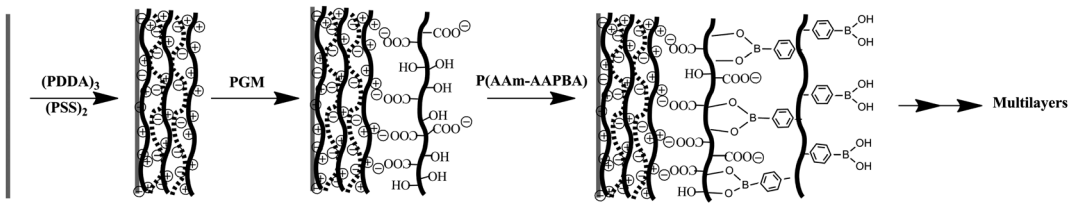

Scheme 1 Schematic illustration of the LbL fabrication of PGM and P(AAm-AAPBA) multilayers.

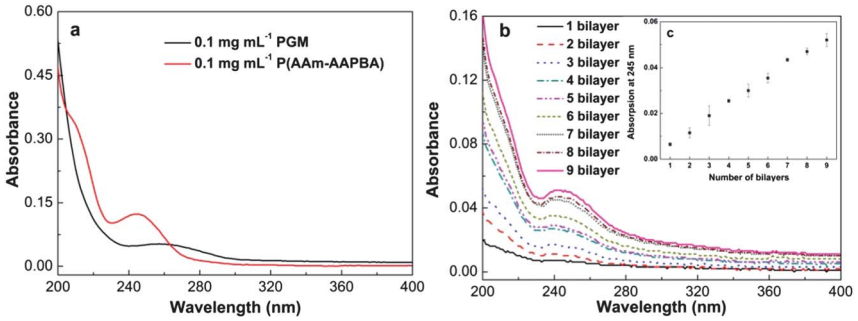

Fig. 2 (a) Absorption spectra for PGM (0.1 mg mL^{-1}, pH 9.0) and P(AAm-AAPBA) (0.1 mg mL^{-1}, pH 9.0) in aqueous solution. (b) Absorption spectra for PGM/P(AAm-AAPBA) films on a silver electrode with different bilayer numbers. (c) The inset shows the step growth of the absorbance at 245 nm as a function of number of bilayers deposited. The films were fabricated in 0.01 M PBS (pH 9.0) containing 0.5 M NaCl.

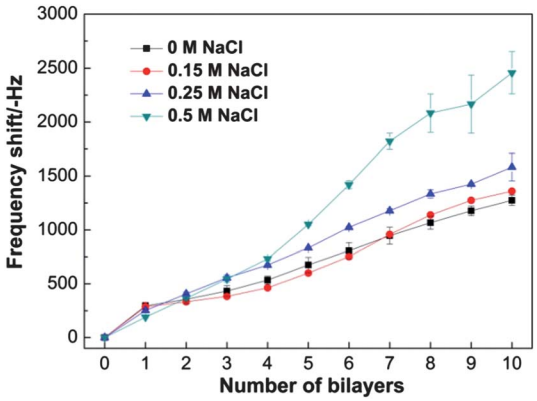

Fig. 3 Frequency shift of PGM/P(AAm-AAPBA) multilayer film dependent on the concentration of NaCl. The concentrations of PGM and P(AAm-AAPBA) were both 0.1 mg mL^{-1} in 0.01 M PBS (pH 9.0).

result in a less extended conformation of the P(AAm-AAPBA), which ultimately gives thicker layer deposition. Additionally, the repulsive interaction between the surface and P(AAm-AAPBA) is reduced as well, which also facilitates the film formation.[24,32]

The films were assembled successfully at pH values ranging from 8.0 to 9.0 as shown in Fig. 4. The deposition trends were similar at pH 8.5 and 9.0. The frequency shifts of the 10-bilayer film fabricated at pH 8.5 and 9.0 were 2171 ± 13 Hz and 2457 ± 195 Hz, respectively. The frequency shift at pH 8.0 was only 415 ± 20 Hz, which was much lower in comparison to the readings at other pH values. The pH-dependent multilayer formation is proposed to be due to the stability of the ester formed between the PBA moiety and the PGM diols. As a weak acid (the pK_a of PBA is 8.8),[43] PBA deprotonates when the pH value increases, which leads to a rising proportion of tetrahedral boronate ion, which is well-known to be able to form stable esters with diols much easier than a planar boronate under less basic conditions.[5] As shown in our results, when the pH is lower than 8.5, there is no efficient active PBA for the fabrication (Fig. 4). This is consistent with the results of a previous report by Levy T. *et al.*[23]

The dependence of multilayer formation on the concentration was also investigated by changing the PGM concentration while keeping the P(AAm-AAPBA) concentration constant. As shown in Fig. 5, with 0.2 mg mL^{-1} and 0.1 mg mL^{-1} PGM, the growth rate and the total adsorption amount of the 10-bilayer film increased by approximately the same degree. With the concentration of 0.02 mg mL^{-1}, the adsorption amount of the assembly film decreased significantly after three deposition cycles. Therefore we fixed the concentrations of PGM and P(AAm-AAPBA) both as 0.1 mg mL^{-1} to fabricate the LbL film in the following studies.

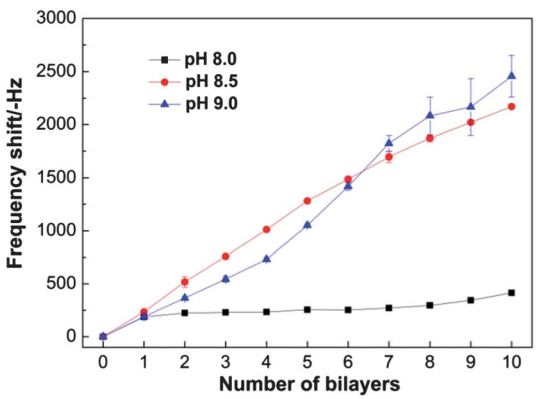

Fig. 4 Frequency shift of PGM/P(AAm-AAPBA) multilayer film under different pH values. The concentrations of PGM and P(AAm-AAPBA) were both 0.1 mg mL^{-1} in 0.01 M PBS containing 0.5 M NaCl.

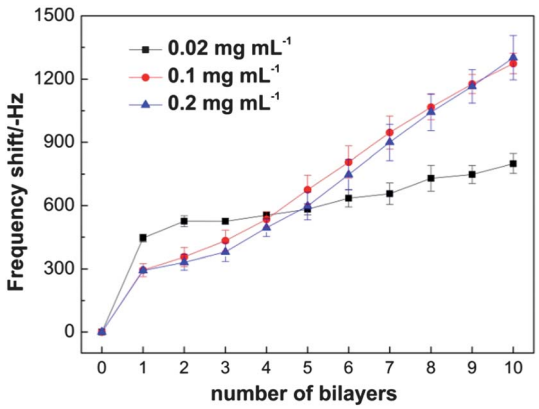

Fig. 5 Frequency shift of PGM/P(AAm-AAPBA) multilayer film dependent on PGM concentration. The concentration of P(AAm-AAPBA) was 0.1 mg mL^{-1} in 0.01 M PBS (pH 9.0).

Dynamic response behavior of PGM and P(AAm-AAPBA) film to glucose

Assembly films with boronate ester as the driving force may disassemble under the appropriate conditions due to the reversibility of the boronate ester bond. For example, the PVA/P(AAm-AAPBA) films can disassemble in glucose solution, in which glucose competes with PVA to bind with PBA groups on the assembly films.[24] In this paper, we investigated the dynamic response of the assembly film with addition of glucose.

Depending on the Sauerbrey equation,[41] the mass desorbed from the surface (Δm) can induce the increase of resonance frequency (Δf) to the crystal sensor. The real-time disintegrating processes of the assembly films were monitored by QCM-D when various concentrations of glucose (0.5 mg mL^{-1}, 1 mg mL^{-1} and 5 mg mL^{-1}, respectively) were added at pH 9.0. The changes in frequency and dissipation *versus* time are shown in Fig. 6. After the stabilization of the baseline in 0.01 M PBS buffer (pH 9.0) in 300 seconds, glucose dissolved in the same buffer was added. As shown in Fig. 6a, the adsorbing process of glucose on the assembly film involves two steps. In the first step, when glucose is adsorbed on the multilayer surface, the frequency decreased around 2.5 Hz, which indicated a similar amount of mass (glucose coupled with water) was adsorbed onto the surface in all cases. In the second step, the change in frequency increased quickly, which indicated the assembly film disassembled from the surface. The disintegration of the assembly film can be regarded as a process to reestablish the equilibrium among the free carbohydrate chains of PGM, the bound carbohydrate chains of PGM and the free PBA groups in the assembly film. The presence of glucose partially consumes free PBA groups, thus the equilibrium shifts to the left hand according to Le Chatelier's principle.[44] In other words, glucose competes with PGM for PBA binding sites and results in disintegration of the assembly film. Apparently, the more glucose present in the solution, the more material disassociates from the assembly film.

The change in dissipation (ΔD) provides more information about the viscoelastic property and structure of the assembled film.[40] The data of ΔD (Fig. 6b) also accord with the disintegrating process. In the first step, a similar amount of glucose adsorbed on the outside surface, which did not change the viscoelasticity of the film much. In the second step, ΔD changed greatly, which indicated glucose was penetrating the assembly film and disturbing the interaction between the PGM and PBA group. In high concentrations of glucose, ΔD was higher, which suggested the assembly films became swollen and much looser. These results indicate that the crosslink density of the assembly film decreases with increasing concentration of glucose. Based on these results, we can conclude that the PGM/P(AAm-AAPBA) film is glucose-sensitive. Furthermore, the results from the present study clearly indicate that the QCM-D can successfully be used to investigate the dynamic response behavior of assembly films in the presence of glucose.

At the same time, we also examined the response of glucose to the assembly film at physiological pH. The baseline was stable in 0.01 M PBS buffer (pH 7.4) in 300 seconds, and then glucose solution (1 mg mL^{-1} in 0.01 M PBS, pH 7.4) was conducted into the flow module. As shown in Fig. 7a, the change of frequency in the first step was negligible, which indicated the adsorbed amount of glucose is low at pH 7.4. This phenomenon clarifies that glucose weakly reacts with PBA units at pH 7.4 compared with the interaction at pH 9.0. It is in agreement with our previous observation that it is difficult to fabricate stable boronate ester at pH value lower than 8.5. In the second step, the frequency shift at pH 7.4 was lower than that at pH 9.0 in the same concentration of glucose (Fig. 7a), which suggested that the pH affected the affinity of PBA toward glucose. This result is in agreement with literature reports that the association constant of the ester formed PBA and glucose increases with increasing pH.[5]

As shown in Fig. 7b, the multilayer film was decomposed in less than 10 min after being exposed to glucose solution (1 mg mL^{-1}), which made the dissipation increase greatly and then reach a relatively steady state. Furthermore, the lower shift of dissipation at pH 7.4 (Fig. 7b) demonstrated that the assembly film was still rigid in the presence of glucose. This result also suggests the interaction between glucose and the PBA moiety is weak at lower pH. On the other hand, the repulsions between inter and intra chains are stronger at pH 9.0 due to more phenylboronate ions in alkaline solution,[43] which results in a floppy conformation and low crosslink density of the assembly film. Y. Zhang, *et al.* reported that microgels using the PBA group as the glucose-sensitive moiety presented glucose-sensitivity only in the range of pH 8.0–9.5, while they showed relatively low sensitivity at pH 7.5.[45] According to these results, we assume that the PGM/P(AAm-AAPBA) film can be disassembled by adding glucose at physiological pH. For further application *in vivo*, we will also investigate the disassembly kinetics of the assembly film

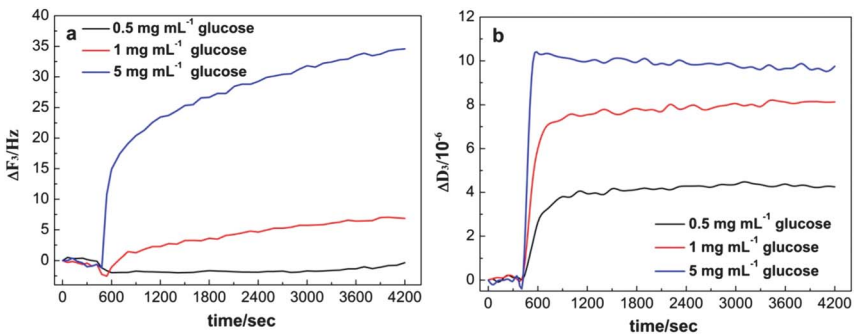

Fig. 6 QCM-D data for the disintegration of PGM/P(AAm-AAPBA) films in various concentrations of glucose at pH 9.0. (a) The corresponding frequency shift *vs.* time for the third overtone. (b) The corresponding dissipation shift *vs.* time for the third overtone.

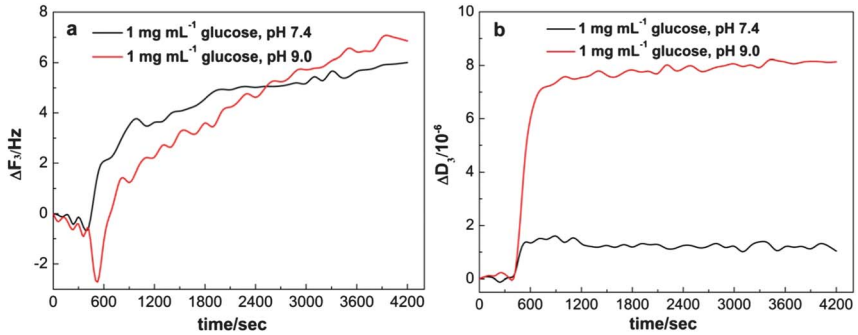

Fig. 7 QCM-D data for the disintegration of PGM/P(AAm-AAPBA) films at pH 7.4 and 9.0. (a) The corresponding frequency shift *vs*. time for the third overtone. (b) The corresponding dissipation shift *vs*. time for the third overtone.

in mimicked physiological conditions including temperature and ionic strength in our future studies.

The above results obtained by QCM-D provide an overall dynamic disintegration of the multilayer film in the presence of glucose. AFM was applied to investigate the morphology of the PGM/P(AAm-AAPBA) film before and after treatment with glucose, in order to understand the disassembly process better. Fig. 8 shows the AFM images of 6-bilayer films at pH 9.0 and 7.4 of the glucose solution (1 mg mL^{-1}) operated in tapping mode. After 6-bilayer adsorption of PGM and P(AAm-AAPBA) the surface was uniformly covered with multilayer films (Fig. 8a). Accordingly, the root mean square roughness (RMS) increased from 0.93 nm for the PDDA substrate surface (Fig. 8d) to 1.64 nm. After the multilayer films were immersed into glucose solution at pH 9.0 and 7.4, the surface RMS increased to 2.59 nm and 2.61 nm, respectively. According to the QCM-D results discussed above, the boronate ester bonds between PGM and PBA groups in the assembly film could almost be broken up in the concentration of 1 mg mL^{-1} glucose at pH 9.0 and 7.4. After washing with water, small pieces of disassembly film were left on the PDDA substrate surface, as shown in Fig. 8b and c, which results in the increasing of surface roughness. Compared to pH 9.0, the disassembling behavior of glucose at pH 7.4 is weaker and slower, so that more disassembly film is left on the substrate after washing. These results agree well with the QCM-D data.

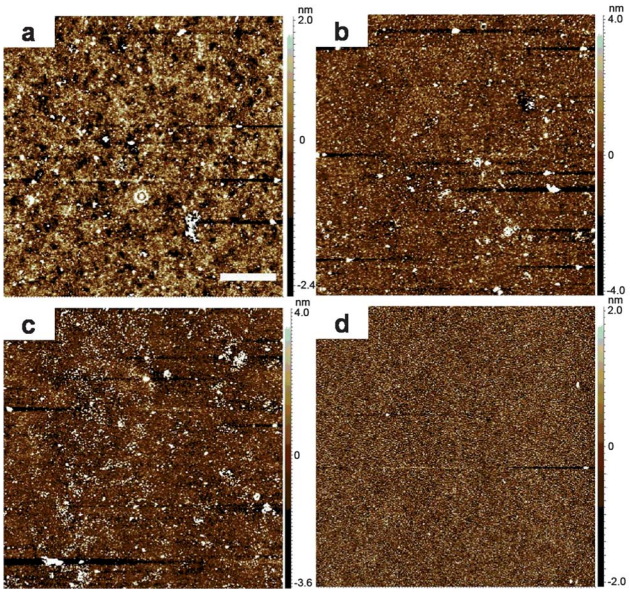

Fig. 8 AFM height images of PGM/P(AAm-AAPBA) multilayer films immersed at two different pH values of the glucose solution. (a) 6-bilayer film without glucose, (b) 6-bilayer film immersed in PBS buffer (pH 9.0) with 1 mg mL^{-1} glucose, (c) 6-bilayer film immersed in PBS buffer (pH 7.4) with 1 mg mL^{-1} glucose and (d) the $(PDDA/PSS)_2$/PDDA film. The image dimensions are 10 × 10 μm^2 and the scale bar is 20 μm.

Conclusions

LbL assembly is a general method to fabricate multilayer films on a solid surface. We demonstrated that a LbL glycoprotein film could be assembled with PGM and P(AAm-AAPBA). The fabricating process of the multilayer film can be influenced by the ionic strength, the concentrations of the two building blocks, and the pH of the solution, which can be monitored by QCM and UV-vis. The adsorption amount of each deposition cycle increased while increasing the ionic strength and pH of the solutions. However, it is difficult to fabricate the multilayer film at pH values lower than 8.5, possibly due to the slower reaction in forming boronate esters between PGM and P(AAm-AAPBA). QCM-D was employed to investigate the real-time dynamic response behavior of the assembly film with addition of glucose. The results indicate that the erosion of the assembly films is accelerated by increasing the glucose concentration at pH 9.0. Moreover, the assembly film is also sensitive to glucose at physiological pH, and the disassembly is slower than that at pH 9.0, which correlates well with the AFM analysis. The results from this study show that the PGM/P(AAm-AAPBA) glycoprotein film may be applied for glucose sensing or self-regulated insulin release systems in a physiological environment.

Acknowledgements

The authors are thankful for financial support from the Chinese Academy of Sciences, and the National Natural Science Foundation of China (Programs 21128002, 21104080). Y.L. and Q.W. also acknowledge the financial support from the State Key Laboratory of Polymer Physics and Chemistry and the Changchun Institute of Applied Chemistry.

References

1 S. Liu, L. Bakovic and A. Chen, *J. Electroanal. Chem.*, 2006, **591**, 210–216.
2 X. Zhang, Y. Wu, Y. Tu and S. Liu, *Analyst*, 2008, **133**, 485–492.
3 X. Ma, H. Li, M. Wu, C. Sun, L. Li and X. Yang, *Sensors*, 2009, **9**, 10389–10399.
4 L. Liang and Z. Liu, *Chem. Commun.*, 2011, **47**, 2255–2257.
5 G. Springsteen and B. Wang, *Tetrahedron*, 2002, **58**, 5291–5300.
6 J. Liu, L. Chen, M. Shih, Y. Chang and W. Chen, *Anal. Biochem.*, 2008, **375**, 90–96.
7 Y. Anraku, Y. Takahashi, H. Kitano and M. Hakari, *Colloids Surf., B*, 2007, **57**, 61–68.
8 P. Liu, Q. Luo, Y. Guan and Y. Zhang, *Polymer*, 2010, **51**, 2668–2675.
9 X. Liu, *Chin. J. Chromatogr.*, 2006, **24**, 73–80.
10 R. Bansil, E. Stanley and J. T. Lamont, *Annu. Rev. Physiol.*, 1995, **57**, 635–657.
11 R. Bansil and B. S. Turner, *Curr. Opin. Colloid Interface Sci.*, 2006, **11**, 164–170.
12 O. Svensson and T. Arnebrant, *Curr. Opin. Colloid Interface Sci.*, 2010, **15**, 395–405.
13 L. Shi, R. Ardehali, K. D. Caldwell and P. Valint, *Colloids Surf., B*, 2000, **17**, 229–239.
14 T. Sandberg, J. Carlsson and M. K. Ott, *J. Mater. Sci.: Mater. Med.*, 2009, **20**, 621–631.
15 G. Decher, *Science*, 1997, **277**, 1232–1237.
16 L. Zhang, M. Zheng, X. Liu and J. Sun, *Langmuir*, 2011, **27**, 1346–1352.
17 X. Wang, L. Zhang, L. Wang, J. Sun and J. Shen, *Langmuir*, 2010, **26**, 8187–8194.
18 X. Zhang, H. Chen and H. Zhang, *Chem. Commun.*, 2007, 1395–1405.
19 Y. Lvov, K. Ariga, I. Ichinose and T. Kunitake, *J. Am. Chem. Soc.*, 1995, **117**, 6117–6123.
20 Y. Lin, Z. Su, Z. Niu, S. Li, G. Kaur, L. A. Lee and Q. Wang, *Acta Biomater.*, 2008, **4**, 838–843.
21 Y. Kobayashi and J. Anzai, *J. Electroanal. Chem.*, 2001, **507**, 250–255.
22 J. Anzai and Y. Kobayashi, *Langmuir*, 2000, **16**, 2851–2856.
23 T. Levy, C. Déjugnat and G. B. Sukhorukov, *Adv. Funct. Mater.*, 2008, **18**, 1586–1594.
24 Z. Ding, Y. Guan, Y. Zhang and X. X. Zhu, *Soft Matter*, 2009, **5**, 2302–2309.
25 K. A. Marx, *Biomacromolecules*, 2003, **4**, 1099–1120.
26 C. I. Cheng, Y. Chang and Y. Chu, *Chem. Soc. Rev.*, 2012, **41**, 1947–1971.
27 T. Sandberg, M. K. Ott, J. Carlsson, A. Feiler and K. D. Caldwell, *J. Biomed. Mater. Res., Part A*, 2009, **91**, 773–785.
28 A. A. Feiler, A. Sahlholm, T. Sandberg and K. D. Caldwell, *J. Colloid Interface Sci.*, 2007, **315**, 475–481.
29 Z. Feldötö, T. Pettersson and A. Dėdinaitė, *Langmuir*, 2008, **24**, 3348–3357.
30 T. J. Halthur, T. Arnebrant, L. Macakova and A. Feiler, *Langmuir*, 2010, **26**, 4901–4908.
31 B. Peng, N. Liu, Y. Lin, L. Wang, W. Zhang, Z. Niu, Q. Wang and Z. Su, *Sci. China: Chem.*, 2011, **54**, 137–143.
32 G. Liu, S. Zou, L. Fu and G. Zhang, *J. Phys. Chem. B*, 2008, **112**, 4167–4171.
33 Y. Yan, G. Liu, Y. Tang and G. Zhang, *Chin. J. Chem. Phys.*, 2008, **21**, 291–294.
34 J. Fatisson, F. Azari and N. Tufenkji, *Biosens. Bioelectron.*, 2011, **26**, 3207–3212.
35 C. Modin, A. L. Stranne, M. Foss, M. Duch, J. Justesen, J. Chevallier, L. K. Andersen, A. G. Hemmersam, F. S. Pedersen and F. Besenbacher, *Biomaterials*, 2006, **27**, 1346–1354.
36 J. Chen, M. Li, L. Penn and J. Xi, *Anal. Chem.*, 2011, **83**, 3141–3146.
37 M. Tagaya, T. Ikoma, T. Takemura, N. Hanagata, M. Okuda, T. Yoshioka and J. Tanaka, *Langmuir*, 2011, **27**, 7635–7644.
38 M. Tagaya, T. Ikoma, T. Takemura, N. Hanagata, T. Yoshioka and J. Tanaka, *Langmuir*, 2011, **27**, 7645–7653.
39 S. Li, E. N. Davis, J. Anderson, Q. Lin and Q. Wang, *Biomacromolecules*, 2009, **10**, 113–118.
40 B. Zhang and Q. Wang, in *Nanotechnology Research Methods for Foods and Bioproducts*, ed. G. W. Padua and Q. Wang, Wiley-Blackwell, Oxford, U.K., 1st edn, 2012, ch. 10, pp. 181–194.
41 G. Sauerbrey, *Z. Phys.*, 1959, **155**, 206–222.
42 M. Rodahl, F. Höök, A. Krozer, P. Brzezinski and B. Kasemo, *Rev. Sci. Instrum.*, 1995, **66**, 3924–3930.
43 J. Yan, G. Springsteen, S. Deeter and B. Wang, *Tetrahedron*, 2004, **60**, 11205–11209.
44 D. J. Evans, D. J. Searles and E. Mittag, *Phys. Rev. E: Stat. Phys., Plasmas, Fluids, Relat. Interdiscip. Top.*, 2001, **63**, 051105.
45 Y. Zhang, Y. Guan and S. Zhou, *Biomacromolecules*, 2006, **7**, 3196–3201.